Available online at www.sciencedirect.com
SCIENCE DIRECT®
Journal of Catalysis 226 (2004) 156–170
JOURNAL OF CATALYSIS
www.elsevier.com/locate/jcat

Reactivity and stability of Au in and on TS-1 for epoxidation of propylene with H_2 and O_2

N. Yap, R.P. Andres, W.N. Delgass *

Purdue University, School of Chemical Engineering, Forney Hall of Chemical Engineering, 480 Stadium Mall Drive, West Lafayette, IN 47907-2100, USA

Received 24 January 2004; revised 8 May 2004; accepted 11 May 2004

Abstract

The direct vapor-phase epoxidation of propylene using hydrogen and oxygen over gold particles prepared by the deposition-precipitation (DP) method on various modified titanium silicalite-1 (TS-1) supports was studied over a reaction time of 24–36 h at a space velocity of 7000 ml g_{cat}^{-1} h^{-1} and temperatures of 413, 443, and 473 K. Gold deposition at pH 9–10 allowed for a consistent amount of 1–3 wt% of the gold available in solution to be deposited, while still maintaining gold particle diameters in the 2–5 nm range, as observed by TEM. These Au/TS-1 catalysts achieved propylene conversions of 2.5–6.5% and PO selectivities of 60–85% at 443 K, with dilute Au and Ti catalysts exhibiting good stability. A key result of the work is that PO rates were not highly influenced by the TS-1 particle size and are thus not proportional to the specific external surface area of the support. The conclusion that activity may reside in the channels of the TS-1 is supported by the finding that the observable gold particles decorating the TS-1 particles only account for ca 30% of the total gold content of the catalyst. Increasing the gold loading up to 0.74 wt% did not increase the PO rates proportionally, suggesting that the active Au–Ti PO-forming centers are limited. In contrast to the prevailing interpretation of this catalyst that a critical Au particle diameter of 2–5 nm is essential for PO activity, our results are consistent with a molecular cluster model where extremely small gold clusters located near Ti sites inside the TS-1 pores or on the external surface are active for propylene epoxidation.

Keywords: Propylene; Epoxidation; Gold; Titanium silicalite-1; Gold clusters; Propylene oxide

1. Introduction

Propylene oxide (PO) is an important chemical intermediate for chemicals like propylene glycol and polyurethanes which are used to manufacture commercial products like adhesives, paints, and cosmetics [1]. Historically, PO is industrially produced by chlorohydrin and hydroperoxidation processes. Both of these processes have disadvantages; the chlorohydrin process produces environmentally unfriendly chlorinated by-products, while the hydroperoxidation process produces stoichiometric amounts of co-products [2]. Most recently, DOW and BASF have utilized a liquid-phase H_2O_2 epoxidation process, catalyzed by titanium–silicalite-1 (TS-1). This process, although ecologically friendly and capable of achieving PO selectivites as high as 98% under optimal conditions, incurrs the cost associated with the use of H_2O_2 [3]. Therefore, it is desirable to produce PO via the direct gas-phase epoxidation of propylene using oxygen, similar to the direct vapor-phase epoxidation of ethylene over Ag/α-Al_2O_3 catalysts. However, the weak allylic hydrogen in propylene and its susceptibility to oxidation have made the direct epoxidation of propylene a grand challenge in the field of catalysis.

The discovery by Haruta and co-workers of Au/TiO_2 catalysts that selectively (> 99%) epoxidize propylene in the presence of propylene, oxygen, and *hydrogen* has opened new doors to the solution of this problem [4,5]. Though highly selective, the Au/TiO_2 catalysts have yet to demonstrate sufficient activity and stability. Continued work on Au supported on TiO_2–SiO_2 and titanosilicates like TS-1, TS-2, TS-β, Ti-MCM-41, and Ti-MCM-48 [6–15] has suggested that the isolation of Ti in tetrahedral sites is a requirement for a stable and active catalyst, motivating us to focus on TS-1 as the catalyst support. The fact that TS-1 successfully catalyzes the production of PO (PO yields 80 to > 98%)

* Corresponding author.
E-mail address: delgass@ecn.purdue.edu (W.N. Delgass).

0021-9517/$ – see front matter
doi:10.1016/j.jcat.2004.05.016

in the presence of H_2O_2 and a solvent [16,17] further adds to this motivation. Two research groups have reported contrasting epoxidation performance for the Au/TS-1 catalyst. Haruta and co-workers reported that their Au/TS-1 catalyst was more selective for propanal than for PO at 473 K, especially if the catalyst was washed thoroughly after gold deposition [9], while Nijhuis et al. [18] did not observe such a product selectivity shift with their 1 wt% Au/TS-1 catalyst. This catalyst achieved a propylene conversion of 1.5% and PO selectivity of 78% at 448 K and a space velocity of 6600 ml h^{-1} g_{cat}^{-1}, or a PO production rate of 20 g_{PO} kg_{cat}^{-1} h^{-1}. An interesting feature of this catalyst was that it did not demonstrate any catalytic deactivation, even after 2 h reaction time. Similar catalyst stability was also reported in the DOW patent where their Au on novel titanium silicate catalysts showed no signs of deactivation even after 68–450 h on stream. These catalysts were also highly selective, at 459–465 K and GHSV of 2069–2105 h^{-1}, they exhibited propylene conversions of 1.5% and PO selectivities of 92%, or PO production rates of 35–37 g_{PO} kg_{cat}^{-1} h^{-1} [19]. The remarkable stability reported for the Au/TS-1 catalyst adds to the potential of this catalyst when compared to a 0.30 wt% Au/Ti-MCM-48 catalyst that achieved initial propylene conversion and PO selectivity of 5.8 and 92%, respectively, at 423 K and a space velocity of 4000 ml h^{-1} g_{cat}^{-1}, or a PO production rate of 55 g_{PO} kg_{cat}^{-1} h^{-1}, but maintained only 60–70% of its activity after 2 h reaction time [13].

Since 1983, Haruta and co-workers have established that the Au–Ti catalyst systems are structurally sensitive at the nanoscale [20]. HRTEM (high-resolution transmission electron microscopy) and HAADF-STEM (high-angle annular dark-field–scanning transmission electron microscopy) have shown that the most active Au–Ti catalysts have hemispherical Au particles in the 2–5 nm region [21]. For epoxidation, Au particles that were smaller than 2 nm were found to be more selective for propane than PO while Au particles that were larger than 5 nm promoted combustion [4,5]. Haruta and co-workers also established that the best method to prepare the Au–Ti catalysts was via the deposition-precipitation (DP) method as this method allowed for production of hemispherical Au particles. Au/TiO_2 catalysts prepared by the impregnation method produced spherical Au particles that only produced CO_2 [5]. Based on these results, Haruta has suggested that the active epoxidation site is the perimeter between the Au particle and the Ti site [21–23], consistent with the higher reactivity observed with hemispherical Au particles. However, since TS-1 has pores of 0.55 nm in size, the Au/TS-1 catalyst offers an alternative site: atomically dispersed gold atoms or clusters near a Ti center inside the zeolite channels. Shape-selectivity experiments, using different-sized olefin reactants, have established the reactivity of these internal Ti centers for the TS-1-catalyzed liquid-phase epoxidation of propylene with H_2O_2 [24]. Clearly, there is also a need to investigate the reactivity of these internal sites for the Au/TS-1 catalyst. In addition to further studying the stability of the Au/TS-1 catalyst, we focus particularly in this paper on the viability of the internal Au–Ti sites for the epoxidation of propylene.

To further pursue the potential of the Au/TS-1 catalyst, we have examined the effect of Si:Ti ratio and Au loading on the activity and stability of the Au/TS-1 catalyst. The Au/TS-1 catalysts presented in this work were prepared by the deposition-precipitation [25] method. Thus far, the controlling DP parameters (DP Au solution concentration and pH) have been reported only for Au deposition on TiO_2 [25]. To ease future preparation of DP Au/TS-1 catalysts, we systematically studied the effects of these parameters for Au deposition on TS-1. To investigate the viability of active internal Au–Ti sites, we compared the catalytic activity of a conventional Au/TS-1 catalyst with gold catalysts made with TS-1 having a particle diameter of 519 nm, more than twice the diameter of our standard material. Due to its larger size, this material has a smaller surface-to-volume ratio than our conventional ∼ 170 nm TS-1 material. Therefore, if the internal Au–Ti sites are not active and the rate scales with external surface area, the 519 nm Au/TS-1 catalyst should demonstrate poorer catalytic performance and the PO rates per gram of catalyst should scale with the reciprocal of the TS-1 particle diameter. The consequences of these kinetic comparisons and the implications of these results on the internal/external reactivity issue are discussed below.

2. Experimental methods

2.1. Synthesis of titanium–silicalite-1 supports

Two types of TS-1 supports were prepared. For the first type, conventional TS-1 with Si:Ti ratios of 35–48 was synthesized according to Ref. [26]. In a typical synthesis, 12.7 ml of a 40 wt% solution of tetrapropylammonium hydroxide (TPAOH, Alfa Aesar) was added dropwise to 24.6 ml of tetraethylorthosilicate (TEOS, Sigma Aldrich) in a polypropylene Erlenmeyer flask with vigorous stirring. Then, 1.1 ml of titanium (IV) butoxide (TBOT, Alfa Aesar) was dissolved in 6.2 ml of isopropanol and stirred. This solution was then added to the TEOS mixture dropwise during vigorous stirring. Finally, another 4.6 ml of TPAOH was added dropwise to the mixture with vigorous stirring, giving a molar composition of 1.000 Si:0.029 Ti:0.300 TPAOH for the resulting synthesis solution. To minimize gelling, all reagents were chilled to 273 K, and the subsequent addition of the reagents was performed with the Erlenmeyer flask in an ice bath. After the addition of all reagents, the mixture was stirred for 30 min and then heated at 353 K for 3 h to remove the solvent (isopropanol). This more viscous mixture was then transferred to a sealed Teflon-lined pressure vessel containing 35 ml deionized (DI) water and heated at 443 K for 24 h to facilitate the crystallization process. The white suspension acquired after the hydrothermal process was washed thoroughly with DI water. To recover the crystals, centrifugation was used instead of filtration because the

particles were too fine to filter. The centrifuged solids were dried in vacuuo at 393 K for 24 h and subsequently calcined in a 20% O_2/He gas mixture at 773 K for 5 h.

The second type of TS-1 support was prepared via the aforementioned procedure except that the resulting synthesis solution had a molar composition of 1.000 Si:0.029 Ti:0.180 TPAOH; i.e., the amount of template was reduced to synthesize TS-1 with larger particle diameters [27]. This larger particle TS-1 material has fewer external framework Ti sites per gram of support (surface-to-volume site ratio, S:V ~ 0.0068), compared to the conventional TS-1 (S:V ~ 0.021). The surface-to-volume site ratios were obtained by using the measured effective TS-1 particle diameters (from TEM) and the known structure of TS-1 to calculate the number of volume sites (# T atoms) and surface sites per TS-1 particle. For this calculation, a framework density of 1.7×10^{28} T atoms/m^3 and surface sites per area of 1.0×10^{19} sites/m^2 were used.

2.2. Deposition of Au onto the TS-1 supports

Au was deposited onto each of the supports using the DP method [25]. In this method, the gold precursor, typically chloroauric acid, $HAuCl_4$, is precipitated as $Au(OH)_3$ on the support by raising the pH. The type of support plays a predominant role on the gold deposition as the support surface acts as a nucleating agent for the selective deposition of the active Au precursor. The DP solution in this work consisted of $HAuCl_4$ (Alfa Aesar, Premion 99.999% metals basis) dissolved in DI water and neutralized to a fixed pH with a 1 M Na_2CO_3 solution. To examine how DP parameters affect Au deposition in TS-1, DP solutions with gold concentrations of 0.98–6.37 wt% and pH of 4–10 were prepared. Then, 130 mg of crushed conventional TS-1 support was mixed with each DP solution, stirred at 298 K for 3 h, washed with 11.5 ml DI water/g support, and centrifuged to recover the solids. The gold samples were dried in vacuuo at 298 K and analyzed by AAS and TEM to determine the resulting gold loadings and particle diameters. Based on the results of these experiments, discussed below, catalysts with gold loadings of 0.06–0.74 wt% and gold particle diameters of 2–7 nm were prepared using DP solutions with gold concentrations of 0.15–0.86 wt% and pH of 9–10. DP procedures for this set of gold catalysts were as noted above except that 1.0 g of crushed support was used, and catalysts were washed with 6–18 ml DI water/g_{cat}.

2.3. Characterization of supports and gold catalysts

The TS-1 supports were characterized by XRD (Siemens D500 Diffractometer, Cu-K_α radiation, 40 kV, 20 mA) to confirm the product identity and DRUV–vis (Perkin Elmer Lambda 40, RSA-PE-20 diffuse reflectance lab sphere) to determine the quality of the supports. TEM (JEOL 2000 FX, 200 keV) was used to obtain the TS-1 and Au particle size and distribution, while the actual Au, Ti, and Si contents in the catalysts were analyzed by AAS (atomic absorption spectroscopy).

2.4. Catalytic activity measurements

Kinetic measurements were carried out in a $\frac{1}{2}$-inch-diameter vertical fixed-bed stainless-steel reactor using a feed concentration of 10/10/10/70 vol% of propylene (99.9%), O_2 (99.9995%), H_2 (99.9995%), and He (99.9995%) at a space velocity of 7000 ml h^{-1} g_{cat}^{-1}. The reaction temperature was controlled and monitored by a K-type thermocouple resting on the top edge of the catalyst bed. Catalysts were sieved to 40–60 mesh prior to kinetic tests to ensure a uniform particle diameter of 250–400 μm. None of the catalysts was pretreated unless otherwise specified. Effluent samples from the reactor were analyzed with a Varian 3740 GC, equipped with an automatic sampling valve. The GC consists of two columns in parallel, each connected to a sample loop. The first column is a Chromosorb 102 packed column (Supelco, length [1.83 m], diameter [3.81 mm]) with a thermal conductivity detector (TCD), while the second column is a fused silica Supelcowax 10 capillary column (Supelco, length [60 m], diameter [0.53 mm], film thickness [1.0 μm]) with a flame ionization detector (FID). Steady-state catalytic activity was tested at three temperatures; 413, 443, and 473 K, with the catalyst remaining at each reaction temperature window for 6 h. Long temperature programs and repeat temperatures, 443–413–473–443 K (26 h) and 443–413–473–443–473–413 K (36 h), were employed to observe the catalyst stability.

3. Results and discussion

3.1. DP experiments: effect of pH and gold concentration

Fig. 1a shows the resulting gold loadings for the series of catalysts prepared using gold solution concentrations of 0.98–6.37 wt% and pH of 4–10, while Fig. 1b shows the wt% of gold available in the solution that was deposited on the support. Unlike similar studies conducted with Au/TiO_2 catalysts [25], there was no optimum pH found for maximum gold loading on TS-1. Instead, the gold loading on the support increased with pH. TEM analysis on samples A and B that were prepared at pH 7 and 10, respectively (Fig. 2), demonstrates that although the particle-size distributions are different for samples A and B, the mean sizes for both samples are between 4 and 5 nm. Thus, the DP pH does not significantly affect the average gold particle diameter on the support. Although not shown in Fig. 2, gold catalysts with Au average diameters of 2–3 nm were also successfully prepared at pH 9–10 when gold solution concentrations of less than 0.5 wt% were used, consistent with observations by Haruta and co-workers that the average Au particle diameters deposited usually decrease with decreasing gold loading [4,5,7]. In accord with this analysis, all gold

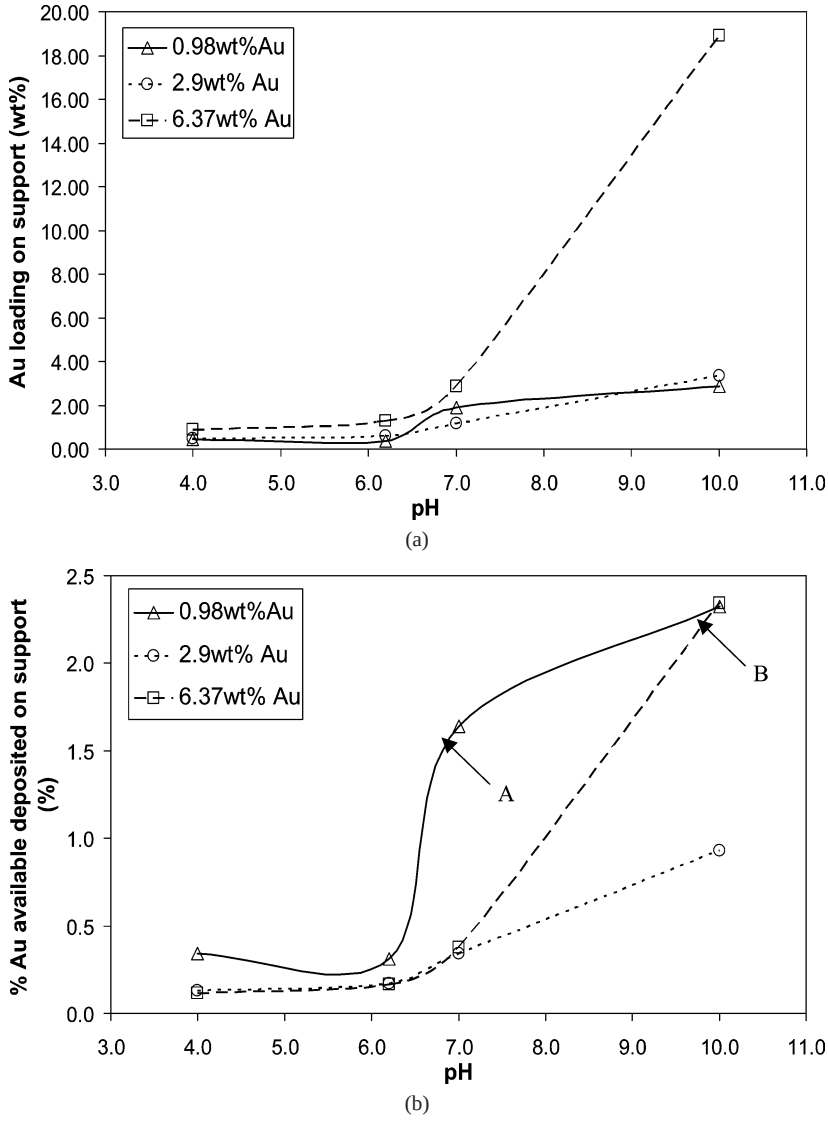

Fig. 1. Dependence of (a) Au loading and (b) % Au available deposited on ∼ 170-nm TS-1 (type 1 support) on gold DP solution concentration and pH.

catalysts in this work were prepared at pH 9–10 because this pH allowed for a maximum amount of gold to be deposited, while still maintaining a small average gold particle diameter of 2–5 nm. At this pH, 1–3 wt% of available gold in the solution was consistently deposited onto the supports. Due to the extremely low Ti content in the TS-1 prepared (1–3 wt% Ti) and the hydrophobicity of the TS-1 material, the amount of gold deposited is significantly lower than the 60 wt% of available gold that was reported to be deposited on Au/TiO_2 at pH 6 by Haruta and co-workers [25].

3.2. Characterization of TS-1 supports and supported gold catalysts

3.2.1. AAS and TEM

For all the gold catalysts studied in this work, Table 1 lists Au loadings and Si:Ti ratios determined by AAS and average TS-1 and gold particle diameters determined from TEM analysis of postreaction samples. At least 20 and 200 particles were averaged to measure the average TS-1 particle diameters and gold particle diameters, respectively, using two image analysis software packages: Optimus Version 6.1 and UTHS CSA Image Tool Version 3.0. Both of these software packages use differences in gray scale to discriminate the particles from the background. However, this method does not allow for a clear resolution of individual gold particles from a cluster of gold particles. Therefore, each cluster of gold particles was magnified, scrutinized, and resolved with the human eye for gold particle diameter measurements. Because the number of gold particles observed on fresh catalysts was small and insufficient for particle averaging, the average gold particle sizes reported in Table 1 were those seen after the kinetic measurements were performed. The gold catalysts are designated by their Au loading, Si:Ti ratio, and TS-1 particle diameter, i.e., 0.16Au/TS1_36_174 corresponds to a 0.16 wt% Au loaded catalyst on a support with a Si:Ti ratio of 36 and particle diameter of 174.

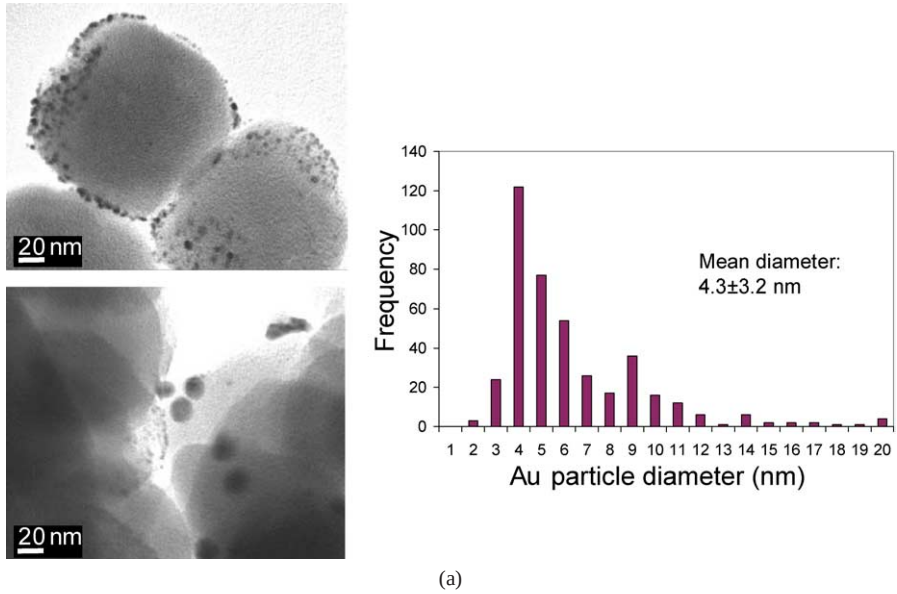

(a)

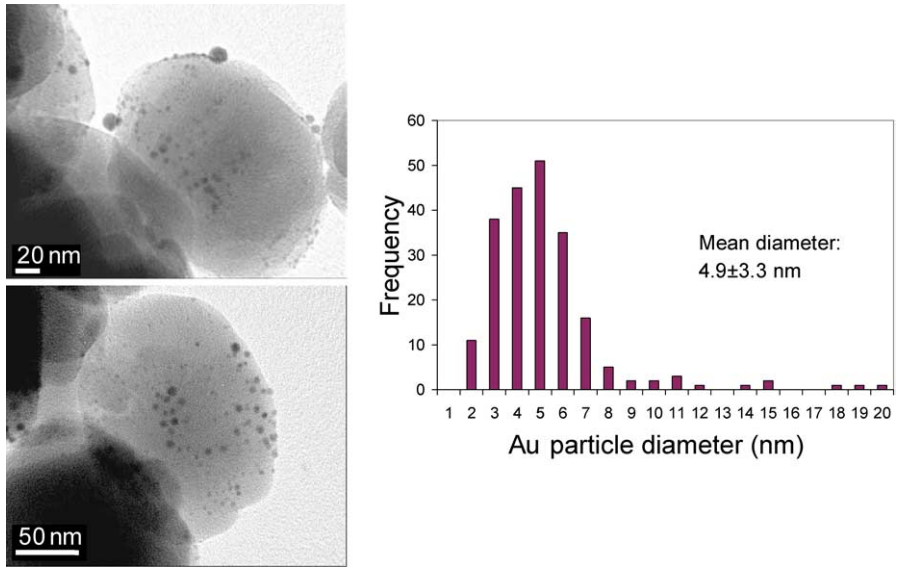

(b)

Fig. 2. TEM analysis for sample A, prepared at pH 7, and sample B, prepared at pH 10, shows little pH effect on the average gold particle diameter.

Table 1
Characterization of gold catalysts

Type	Catalyst	Si:Ti	D_{TS-1} (nm)	Au loading (wt%)	D_{Au} (nm)
1	0.06Au/TS1_48_162	48	161.9 ± 22.9	0.06	3.06 ± 2.25
	0.07Au/TS1_36_165	35	165.4 ± 36.7	0.07	4.23 ± 3.96
	0.14Au/TS1_48_162	48	161.0 ± 22.9	0.14	2.12 ± 0.69
	0.16Au/TS1_36_174	36	173.8 ± 33.2	0.16	3.93 ± 1.91
	0.21Au/TS1_35_165	35	165.4 ± 36.7	0.21	3.13 ± 1.47
	0.25Au/TS1_36_174	36	173.8 ± 33.2	0.25	3.72 ± 2.97
	0.26Au/TS1_36_174	36	173.8 ± 33.2	0.26	3.25 ± 2.21
	0.52Au/TS1_48_162	48	161.9 ± 22.9	0.52	4.47 ± 2.47
	0.63Au/TS1_36_152	36	152.4 ± 36.7	0.63	4.13 ± 2.07
	0.72Au/TS1_36_152	36	152.4 ± 36.7	0.72	3.07 ± 1.25
	0.74Au/TS1_36_152	36	152.4 ± 36.7	0.74	3.14 ± 1.74
2	0.06Au/TS1_33_519	33	518.6 ± 83.1	0.06	6.15 ± 4.41
	0.11Au/TS1_33_519	33	518.6 ± 83.1	0.11	4.01 ± 2.94
	0.31Au/TS1_33_519	33	518.6 ± 83.1	0.31	6.74 ± 2.09

Fig. 3 shows typical TEM images of the support particles, indicating homogeneous berry-like particles with average particle diameters of 150–175 and 519 nm. Fig. 4 shows typical TEM images of the gold catalysts made from the two different TS-1 supports. These images were taken after kinetic measurements were performed and show a dispersion of Au with average particle diameters of 2–5 nm for the 150- to 175-nm supports, and 4–7 nm for the 519-nm support.

3.2.2. XRD and DRUV–vis

The structures of the two different types of TS-1 supports prepared were confirmed by XRD. Fig. 5 shows that the supports are highly crystalline TS-1 with the MFI structure [28–30]. The incorporation of Ti^{IV} into the framework is indicated by the conversion of the monoclinic structure of silicalite-1 to an orthorhombic structure, evidenced by the

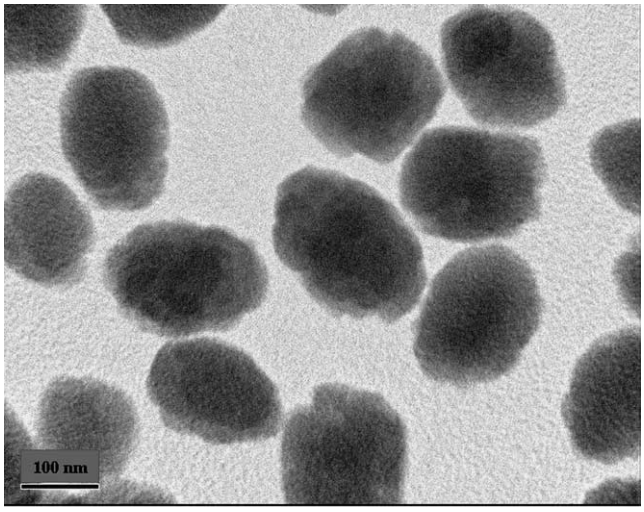

(a) TS1_36_174

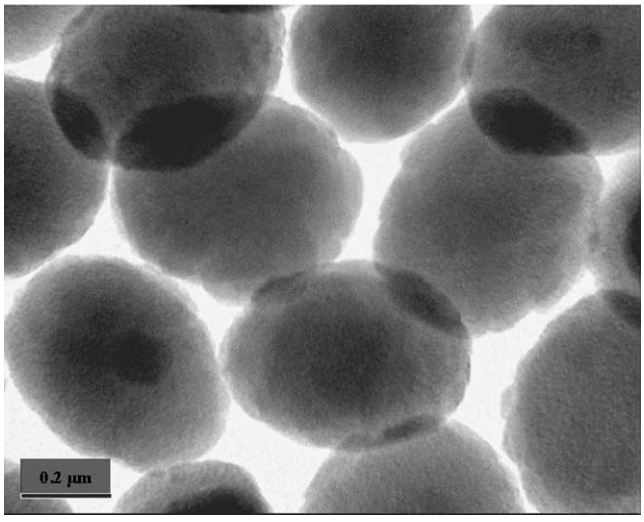

(b) TS1_33_519

Fig. 3. TEM micrographs of (a) ∼ 170-nm conventional TS-1 (type 1) and (b) 519-nm large particle TS-1 (type 2) supports.

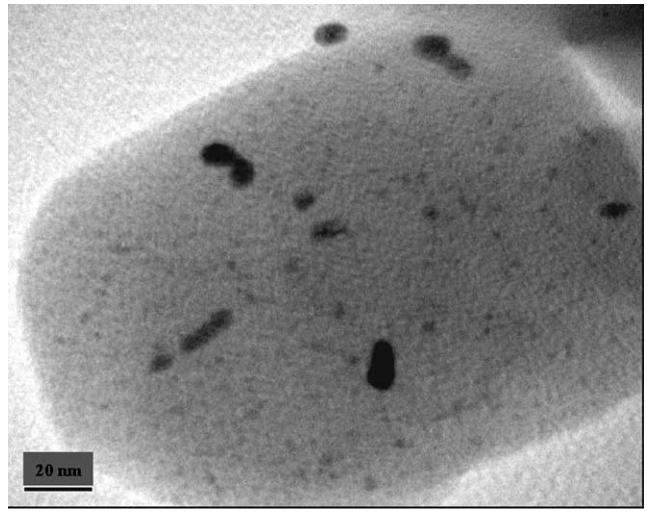

(a) TS1_36_174

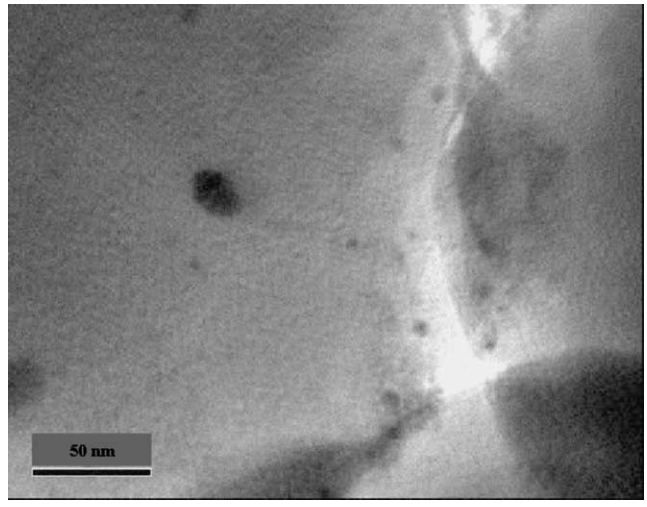

(b) TS1_33_519

Fig. 4. TEM micrographs of (a) ∼ 170-nm (type 1) and (b) 519-nm (type 2) Au/TS-1 catalysts after kinetic measurements.

disappearance of peak splittings at $2\theta = 24.5°$ and $2\theta = 29.5°$ [30], marked with arrows on Fig. 5. Because of the low Ti content in the support materials (Ti < 3 wt%), additional TiO_2 crystalline phases, i.e., anatase ($2\theta = 25.5°$) and rutile ($2\theta = 48.2°$), were not identified in the XRD patterns.

Excess of anatase and/or extraframework Ti in Au–Ti catalysts has been reported to be the cause of catalyst deactivation; these dense octahedral Ti sites accelerate PO oligomerization, which subsequently blocks the active sites [5,18,31]. Since anatase and/or extraframework Ti are normally present in TS-1 samples that have greater than 2.5 at.% Ti (Si:Ti < 39) [32–34], the quality of our TS-1 samples was determined by DRUV–vis spectroscopy. DRUV–vis spectra of silicalite-1 and the two different types of TS-1 samples prepared, Fig. 6, show that isolated tetrahedral framework Ti^{IV} centers are evident in our TS-1 samples, evidenced by strong absorptions at 209–220 nm [28–30]. For a clearer distinction, the DRUV–vis spectra shown in Fig. 6a are at an offset. This figure confirms that, consistent with literature, anatase phases (peak at 320–340 nm) were only present for the TS-1 sample with the lower Si:Ti ratio (Si:Ti = 35). Fig. 6b shows that a weak 260-nm absorption (indicated by arrow), attributed to Ti in an octahedral environment, was observed for TS1_33_519, indicating that extraframework Ti is present in this sample.

3.3. Propylene epoxidation over Au/TS-1 catalysts

3.3.1. Catalyst stability: Si:Ti ratio and Au loading effect

Catalyst instability is a problem for the Au–Ti catalyst systems. The activity of Au/TiO_2 catalysts decreases with time on stream after 10–20 min [4,5] and can diminish by 50% in 2 h [18]. Stability has been improved by isolating the Ti sites; using catalyst supports like TS-1, and Ti-MCM materials that have dispersed, tetrahedral Ti sites and have a limited amount of TiO_2 (anatase) phases [7,14,15]. This

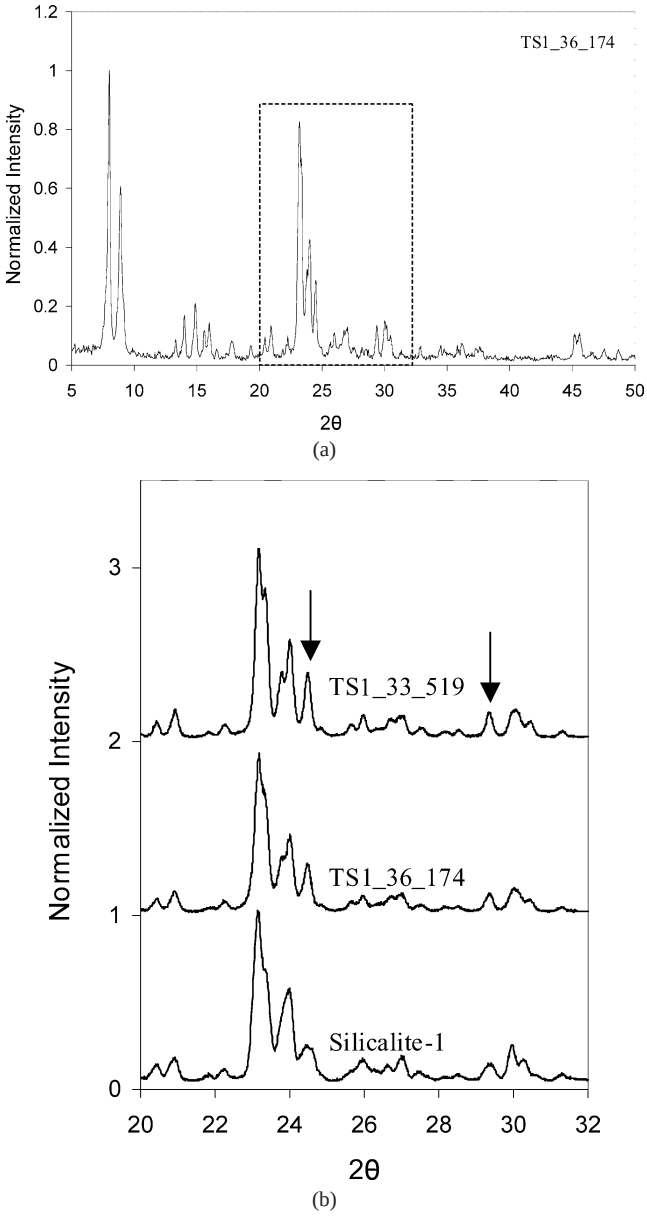

Fig. 5. XRD patterns of silicalite-1 and the two different types of TS-1 supports: ∼ 170-nm conventional TS-1 (type 1), and 519-nm large particle TS-1 (type 2).

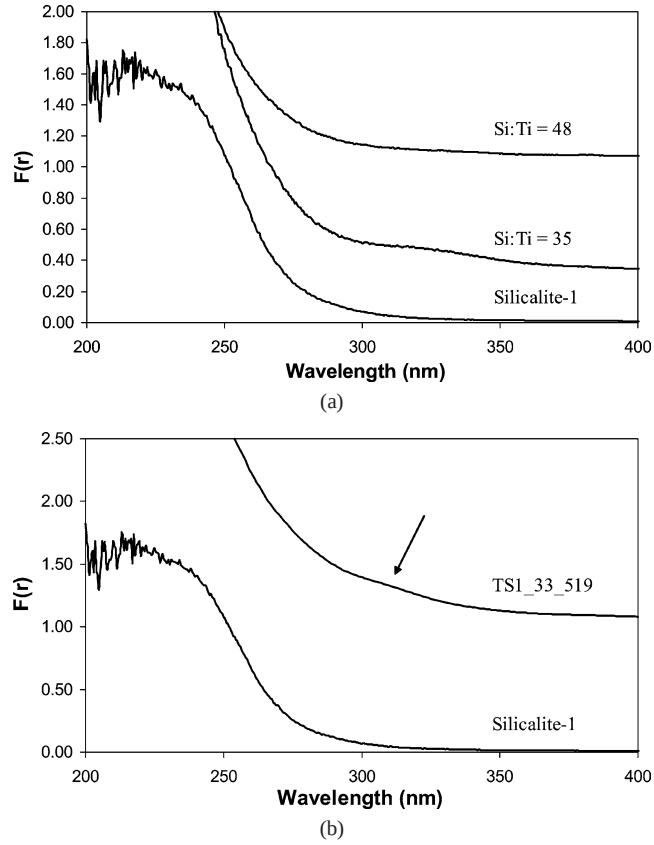

Fig. 6. DRUV–vis spectra of the two different types of TS-1 supports: (a) ∼ 170-nm conventional TS-1 (type 1) with varied Si:Ti ratios and (b) 519-nm large particle (type 2) TS-1.

improvement has led to the hypothesis that PO oligomerization on Ti sites that are in close proximity could be the cause of catalyst instability [5,18,31]. Catalyst deactivation could also be caused by secondary reactions of PO on silanol groups present on the exterior and interior channels of TS-1 [35,36]. However, since catalyst stability has been demonstrated to be quite dependent on Si:Ti ratio and the presence of anatase phases, it is more likely that the effect of the silanol groups on catalyst deactivation is weaker than that of the effect of Ti loading and the presence of octahedral Ti. Interestingly, although both TS-1 and Ti-MCM-41 materials have dispersed tetrahedral Ti sites, the excellent catalyst stability observed by Nijhuis et al. [18] with their Au/TS-1 catalyst was not observed on the Au/Ti-MCM materials by Haruta and co-workers [7,8,11,13], suggesting that factors in addition to high octahedral Ti content contribute to catalyst instability. Since high Au loading accelerates Au particle sintering, which subsequently promotes combustion, high Au loading could be such a factor.

In this work, we studied the epoxidation performance of Au/TS-1 catalysts with gold loadings of 0.06–0.74 wt% and Si:Ti ratios of 33–48. The steady-state activities of these catalysts at 413, 443, and 473 K are presented in Table 2. To examine the stability of the catalysts, besides obtaining steady-state kinetic data at various temperatures, we also monitored the catalyst activity as a function of reaction time. The effect of Au loading and Si:Ti ratio on catalyst stability was studied by comparing the kinetic trends of two catalysts over a 36-h period (Fig. 7). The first is a catalyst with low Au loading, but high Si:Ti ratio, 0.14Au/TS1_48_162, while the second is a catalyst with high Au loading but low Si:Ti ratio, 0.74Au/TS1_36_152. As discussed, DRUV–vis spectroscopy shows the TS-1 materials with low Si:Ti ratios (Si:Ti < 39) to have an anatase phase and/or extraframework Ti (Ti in octahedral environment). Fig. 7 shows that the catalyst with low Au loading but high Si:Ti ratio, 0.14Au/TS1_48_162, demonstrated remarkable catalyst stability; this catalyst showed no signs of

Table 2
Activity and selectivity of gold catalysts

Catalyst	413 K		443 K		473 K	
	C_3H_6 conversion (%)	PO selectivity (%)	C_3H_6 conversion (%)	PO selectivity (%)	C_3H_6 conversion (%)	PO selectivity (%)
0.06Au/TS1_48_162	1.4	60	2.7	60	4.1	54
0.07Au/TS1_36_165	1.2	87	2.7	82	4.3	67
0.14Au/TS1_48_162	1.6	78	3.3	74	5.1	66
0.16Au/TS1_36_174	2.3	85	4.6	78	6.1	53
0.21Au/TS1_35_165	1.7	84	3.3	80	5.0	62
0.25Au/TS1_36_174	3.0	84	4.4	79	5.9	60
0.26Au/TS1_36_174	2.3	84	4.2	75	5.7	51
0.52Au/TS1_48_162	2.9	76	6.2	71	7.5	33
0.63Au/TS1_36_152	2.3	76	4.7	70	6.4	54
0.72Au/TS1_36_152	2.9	71	5.7	63	7.5	42
0.74Au/TS1_36_152	2.9	75	5.5	67	7.2	51
0.06Au/TS1_33_519	1.0	84	2.4	76	4.0	58
0.11Au/TS1_33_519	1.7	86	3.8	80	5.6	58
0.31Au/TS1_33_519	2.3	84	5.3	77	6.8	51

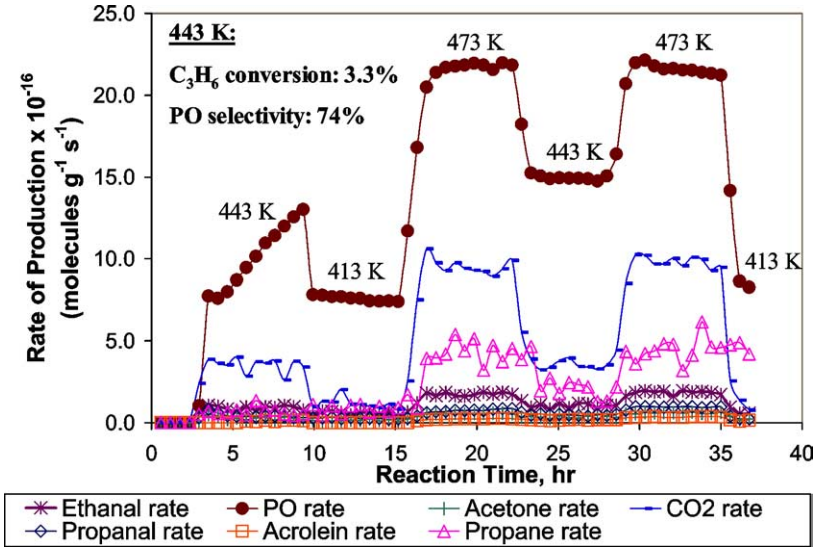

(a)

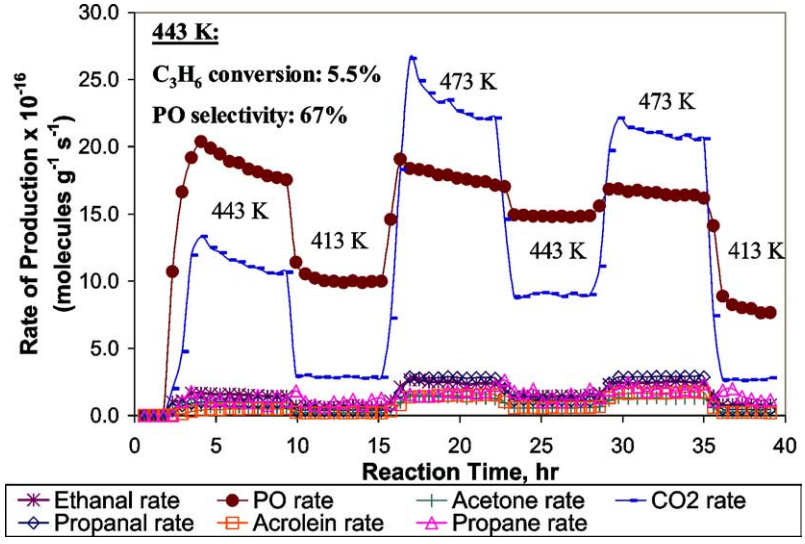

(b)

Fig. 7. Catalytic performance as a function of reaction time for (a) 0.14Au/TS1_48_162 and (b) 0.74Au/TS1_36_152 over a 36-h period at 413, 443, and 473 K. Steady-state C_3H_6 conversion and PO selectivity shown refer to the first 443 K temperature window for (a).

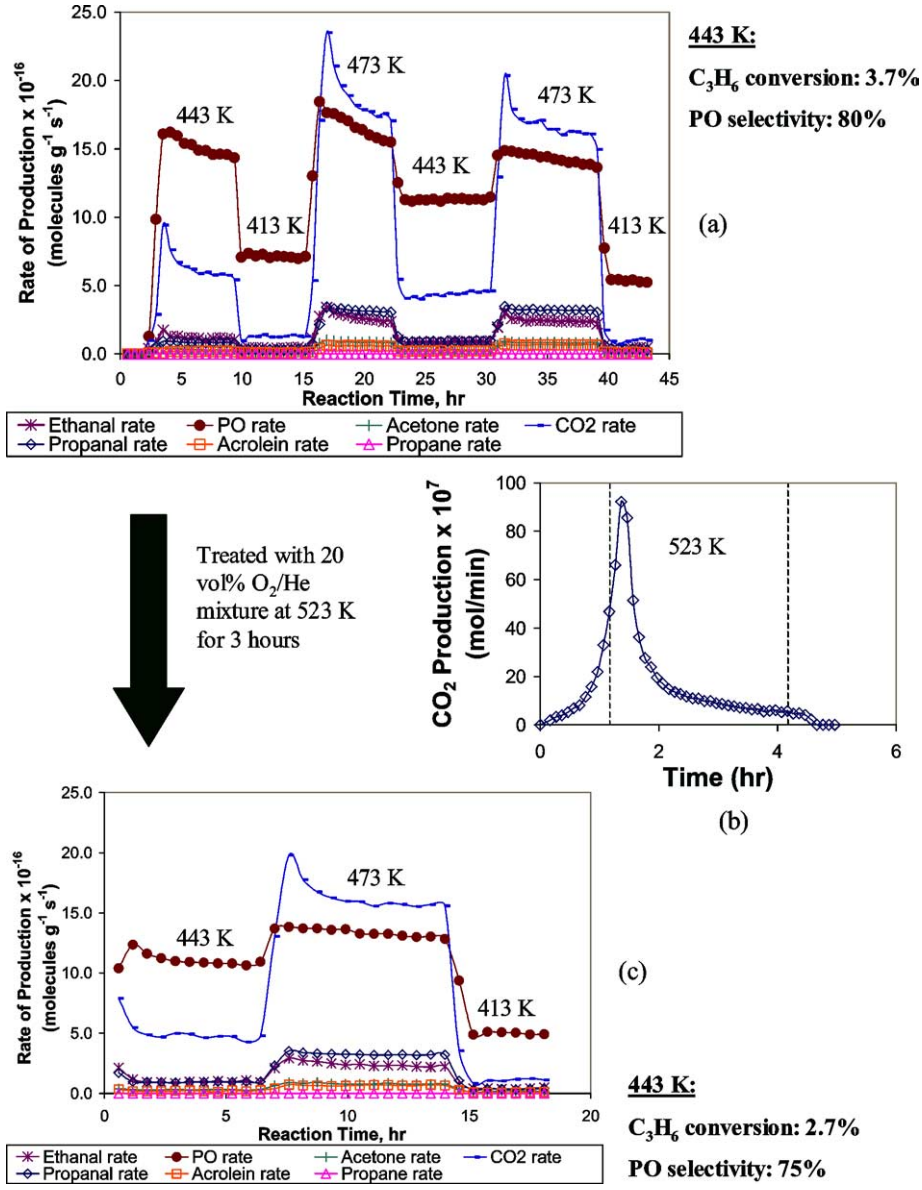

Fig. 8. Effect of 20 vol% O_2/He treatment on 0.11Au/TS1_33_519; (a) initial catalytic performance as a function of reaction time; (b) tracking of CO_2 combustion during 20 vol% O_2/He treatment; and (c) catalytic performance as a function of time after the 20 vol% O_2/He treatment. Steady-state C_3H_6 conversion and PO selectivity shown refer to the second 443 K temperature window for (a) and the first 443 K temperature window for (b).

deactivation and yielded the same PO activities when the reaction temperature sequence was repeated. A long induction period was also observed for this catalyst. However, a similar induction period was not observed for a similar Au loaded catalyst with a lower Si:Ti ratio, 0.16Au/TS1_36_174 (Fig. 9), suggesting that the small amounts of both Ti and Au in 0.14Au/TS1_48_162 may increase the diffusion lengths needed for Au to find Ti centers to form the active sites. During pretreatment, migration of Au to form gold particles was seen in TEM analysis, which showed the emergence of gold particles after 0.16 Au/TS1_36_174 was pretreated with a 20% O_2/He mixture at 543 K for 3 h. Prior to pretreatment, no gold particles were observed on the fresh samples. The pretreated 0.16 Au/TS1_36_174 also activated more rapidly than the untreated catalyst; i.e., at 2.3 h on stream, the rates of PO production were 8×10^{16} and 2×10^{16} molecules/(g s), respectively, for the pretreated and untreated catalyst.

A long induction period was not observed for a catalyst with high Au loading but low Si:Ti ratio, 0.74Au/TS1_36_152. Instead, this catalyst gave an activity spike at the beginning of the reaction, but later showed a degradation in catalytic performance with time. This result suggests that dilute Au and Ti loading are essential for catalyst stability, but does not confirm if low Si:Ti ratio and/or high Au loading is the cause of catalyst deactivation. We further examined these two factors by performing two experiments. First, to check if the carbon formed on the catalyst surface during reaction

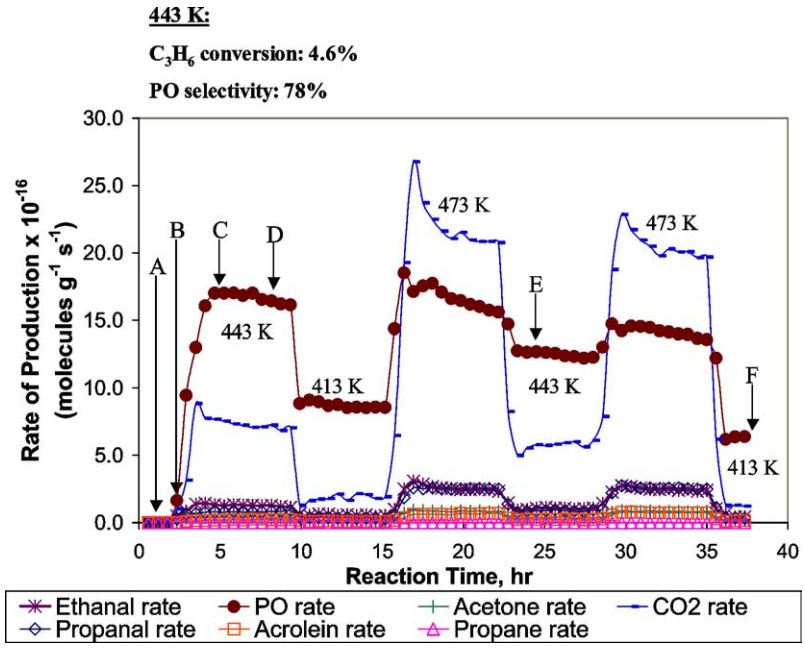

Fig. 9. Catalytic performance as a function of reaction time for 0.16Au/TS1_36_174. Steady-state C_3H_6 conversion and PO selectivity shown refer to the second 443 K temperature window for (a) and the first 443 K temperature window for (b). A, B, C, D, E, and F represent the different times when the catalyst was quenched for TEM analysis.

(caused by PO oligomerization) was sufficient to poison the active PO-forming sites, we determined the total amount of carbonaceous material that accumulated on the surface of a catalyst that had exhibited catalyst degradation with time. This catalyst, 0.11Au/TS1_33_519, has a relatively low Au loading and Si:Ti ratio. Second, to determine if the gold particles had sintered under reaction conditions, we tracked the growth of the gold particles during reaction. This particle progression experiment was performed on two catalysts, the first, 0.16Au/TS1_36_174, has a low Au loading and Si:Ti ratio while the second, 0.52Au/TS1_48_162, has a high Au loading and Si:Ti ratio.

As noted above, high extraframework Ti content (low Si:Ti ratio) accelerates PO oligomerization on the catalyst surface, which could subsequently block potential active epoxidation sites. Carbonaceous material was observed by Nijhuis et al. [18] to be a source of deactivation on their Au–Ti catalysts using thermogravimetric analysis (TGA) in synthetic air. Although they observed two types of carbonaceous materials, one that combusted at 500 K and another that combusted at 600 K, they attributed only the first material to be the catalyst-poisoning compound as catalyst deactivation was not observed on used Au–Ti catalysts that contained the 600 K carbonaceous material. To examine whether PO oligomerization was the cause of catalyst deactivation for our Au/TS-1 catalysts, we treated 0.11Au/TS1_33_519 with a 20 vol% O_2/He mixture at 523 K (above the combustion temperature of the catalyst-poisoning compound observed by Nijhuis et al. [18]) for 3 h after the standard kinetic measurements were performed. During this treatment, the carbon burnoff (CO_2 production) was tracked with a TCD detector every 6 min (Fig. 8b). Fig. 8a shows the 36-h kinetic trend of 0.11Au/TS1_33_519 which demonstrated catalyst deactivation with time, while Fig. 8c shows no improvement in catalyst activity after the O_2/He treatment. Similar unsuccessful catalyst regeneration efforts were also observed by Haruta and co-workers [12,13] and Nijhuis et al. [18] on Au/Ti-MCM and Au/TiO_2 catalysts. The total carbon burnoff during the O_2/He treatment was calculated to be approximately 1.55 mmol/g_{cat}. Based on the fact that 0.11Au/TS1_33_519 has a Ti loading of 2.10 wt%, a total of 3 C per Ti site was obtained if the carbon cokes all the Ti sites, while a higher number of 400 C per Ti site was obtained if the carbon only cokes the external Ti sites. However, since not every external Ti site is interacting with a gold particle, if all the gold in 0.11Au/TS1_33_519 forms 4-nm gold particles, the C atom:Au particle ratio is approximately 3×10^5 atoms/particle. This quantitative analysis clearly indicates that the carbon that was removed by the O_2/He treatment could sufficiently coke and poison the possible Au and Ti sites. However, as the activity was not restored by this treatment, it is quite possible that the reaction or the O_2/He treatment conditions caused irreversible rearrangement of the active Au and/or that the catalyst-poisoning material was not fully removed at 523 K.

To determine if gold particle sintering could contribute to catalyst instability, the progression of the gold particle-size distribution throughout the reaction time was studied for 0.16Au/TS1_36_174 which deactivated with time despite its low Au loading. As shown in Fig. 9, the reaction was quenched at various times on stream for six separate samples: A (1 h), B (2.5 h), C (3.5 h), D (7.3 h), E (24 h), and F (36 h). TEM analysis was then performed on those catalyst samples to determine the size of the gold particles. The

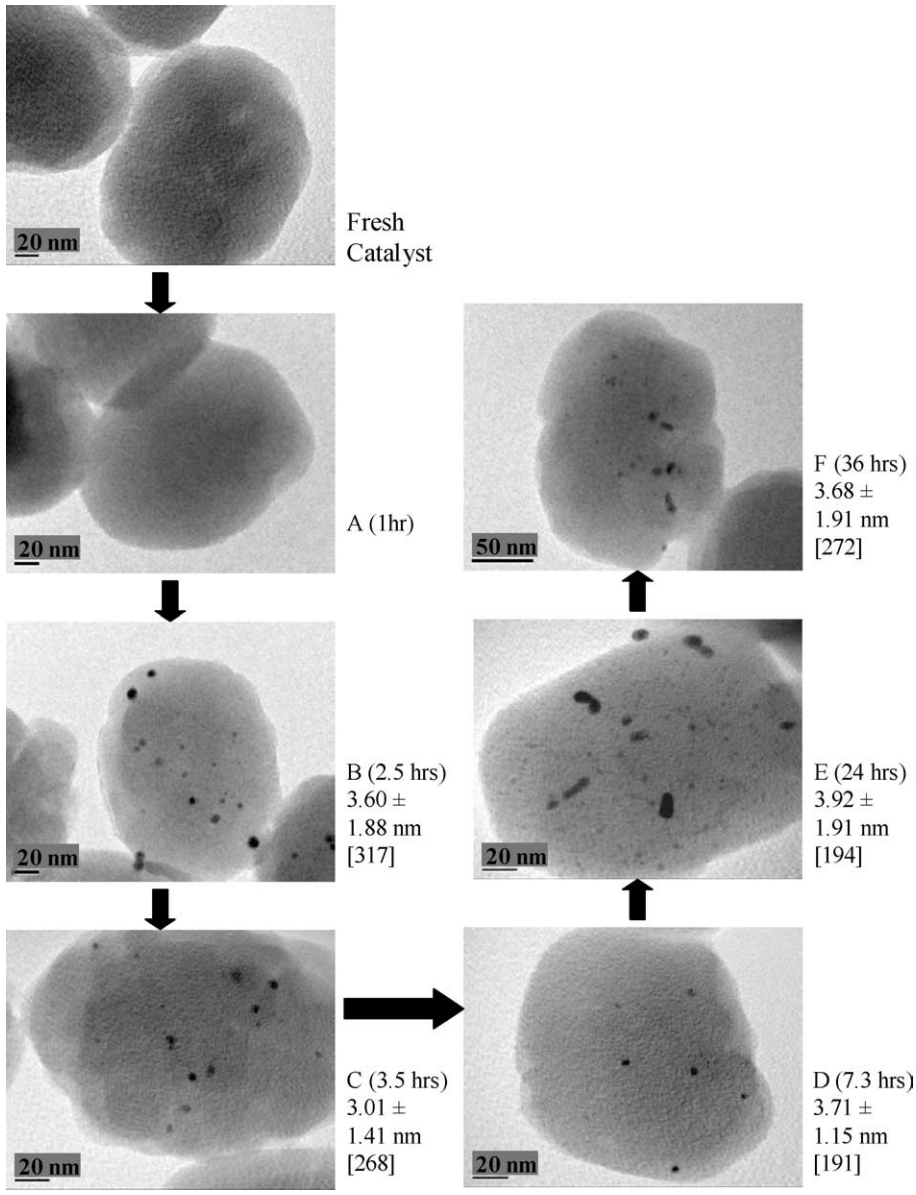

Fig. 10. TEM images to show the progression of gold particles throughout a 36-h reaction time period for 0.16Au/TS1_36_174. Number of particles used for average particle diameter measurements is shown in brackets.

progression of TEM images and gold particle diameters for this experiment is shown in Fig. 10. The results confirm that for this low gold loaded catalyst, the gold particles, formed by the initial reaction exposure, did not grow during reaction. Thus, catalyst instability observed for this catalyst was not caused by sintering of gold particles large enough to be seen with TEM.

The particle progression experiment was also performed on a higher gold loaded catalyst, 0.52Au/TS1_48_162, where catalyst samples were quenched at three reaction times; A (4 h), B (7.5 h), and C (27 h). The kinetic trend and particle-size progression of this catalyst are shown in Fig. 11. After 4 and 7.5 h on stream, the gold particle-size remained much the same. However, after 27 h, more gold particles per TS-1 particle were observed. Large agglomerates of gold particles were also observed giving a larger average gold particle diameter of 4.47 ± 2.47 nm. This result suggests that although sintering of observable gold particles is not the cause of catalyst instability for low gold loaded catalysts, such is not the case for catalysts loaded with more than 0.5 wt% gold. As observed in Fig. 11a, the CO_2 rate at 473 K increased at the expense of PO rate, indicating that some of the gold that was initially active for PO has converted into larger gold particles that are more active for combustion. The appearance of more gold particles decorating the TS-1 support after 27 h, Fig. 11b, suggests the possibility that reaction conditions caused the migration of atomic Au (not observable by TEM) from either internal or external sites to form observable gold particles at the exterior of the TS-1 crystallites.

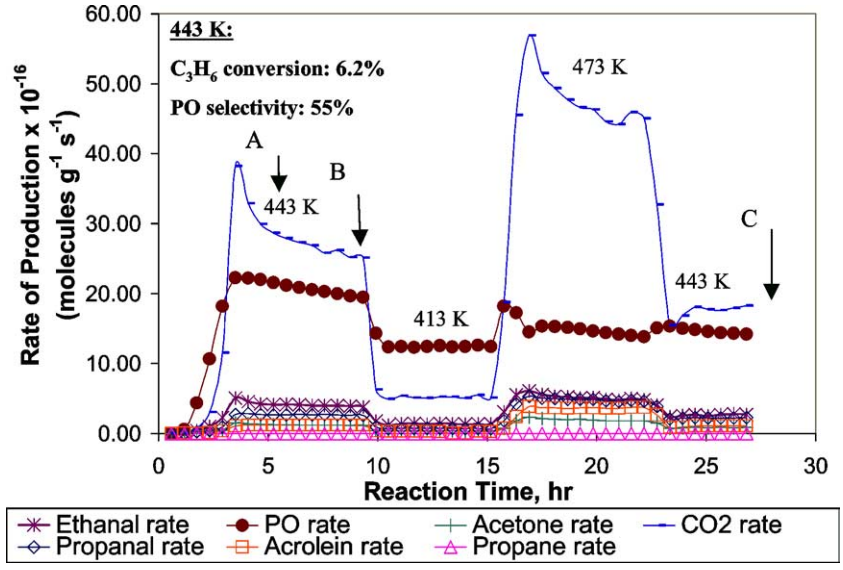

(a)

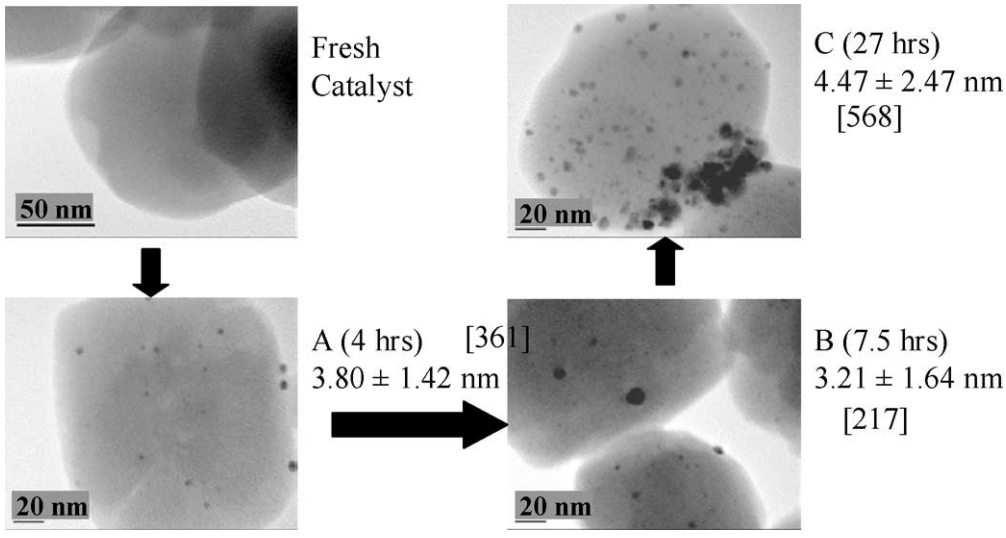

(b)

Fig. 11. (a) Catalytic performance as a function of reaction time for 0.52Au/TS1_48_162. Steady-state C_3H_6 conversion and PO selectivity shown refer to the second 443 K temperature window. A, B, and C represent the different times when the catalyst was quenched for TEM analysis, (b) TEM images to show the progression of gold particles throughout a 27-h reaction time period (samples A through C). Number of particles used for average particle diameter measurements is shown in brackets.

3.3.2. Reactivity and stability of atomically dispersed internal Au–Ti sites

To further probe the possibility of active internal Au–Ti sites, the PO rates of Au/TS-1 catalysts were compared for gold catalysts with different surface-to-volume ratios resulting from different TS-1 particle diameters. The ∼ 170-nm TS-1 particles have a larger surface-to-volume site ratio (S:V ∼ 0.021) than the 519-nm TS-1 particles (S:V ∼ 0.0068). Therefore, if epoxidation is proportional to the number of external framework Ti sites, the PO rate per gram of catalyst for the larger diameter catalyst should be approximately 3.1 times (0.021/0.0068) lower than that for the ∼ 170-nm catalyst. On the other hand, if the active sites are uniformly distributed in the volume of the catalyst, the rates would be unchanged by the TS-1 particle diameter.

Fig. 12 compares the PO and CO_2 TOFs for catalysts with TS-1 particle diameters of ∼ 170 and 519 nm at three gold loadings: ∼ 0.07 wt% Au, ∼ 0.1 wt% Au, and ∼ 0.3 wt% Au. The TOFs were calculated by normalizing the rates of production to the total Au content. The kinetic measurements show that the PO and CO_2 TOFs are not greatly influenced by the TS-1 particle diameters. The largest difference in PO TOF was observed for the ∼ 0.1 wt% Au catalysts, Fig. 12b, at 473 K. However, this result does not support the external surface activity argument since the PO TOF for the larger particle catalyst demonstrates the higher activity. The PO TOFs for the ∼ 170- and 519-nm catalysts initially start out similar at 413 K. Thus, the larger disparity at 473 K is attributed to more pronounced catalyst deactivation or loss of Au–Ti sites at higher temperatures for 0.16Au/TS1_36_174.

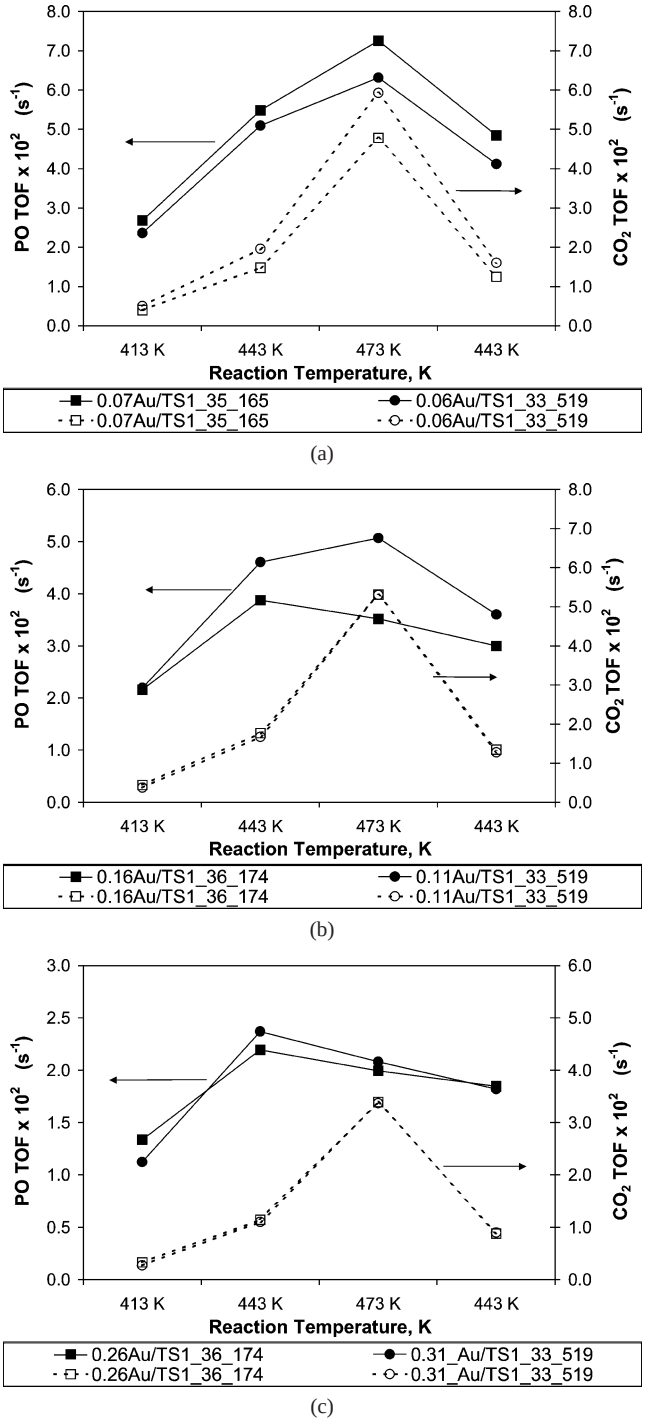

Fig. 12. PO and CO_2 TOFs for three groups of catalysts with varied TS-1 particle diameters: (a) ∼ 0.07 wt% Au loading, (b) ∼ 0.1 wt% Au loading, and (c) ∼ 0.3 wt% Au loading.

A linear regression analysis on the PO rates as a function of several experimental parameters varied in this work (Au loading, reaction temperature, Si:Ti ratio, and TS-1 particle size) also showed that the TS-1 particle size demonstrated the least influence on catalyst activity, consistent with catalyst activity uniformly distributed in the volume of the catalyst particles. However, this result only disfavors the external

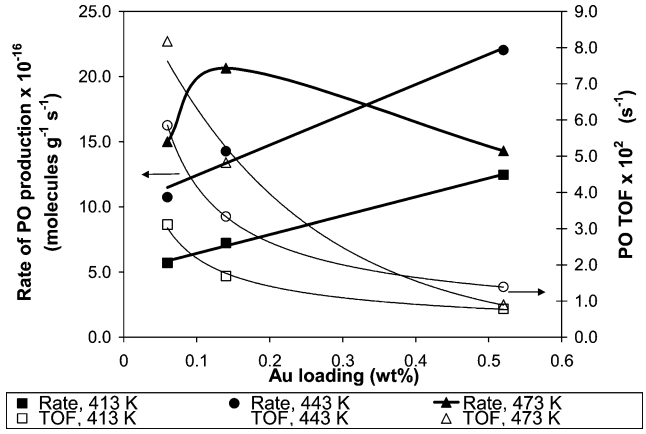

Fig. 13. PO rates as a function of Au loading at 413, 443, and 473 K for conventional Au/TS-1 catalysts with Si:Ti ratio of 48.

site model and does not require that the active sites are exclusively internal.

Since higher temperatures increase PO rate and mitigate poisoning by PO inhibition, stability of these catalysts at high temperature is an important factor. For our conventional Au/TS-1 catalysts that have no extraframework Ti (Si:Ti = 48), Fig. 13 shows that the PO rates do increase with Au loading at 413 and 443 K. At 473 K, the PO rate initially starts to increase with Au loading, but drastically drops at ∼ 0.5 wt% Au loading, consistent with the instability of the Au–Ti PO-forming sites under these conditions. Therefore, for the "clean" (no extraframework Ti) materials, both high Au loading and high temperature conditions contribute to catalyst instability. It is possible that these extreme conditions accelerate the migration of atomic Au to coalesce and form gold particles at the external Ti sites which are less active for PO formation. When we studied the activity of our conventional Au/TS-1 catalysts that have extraframework Ti content (Si:Ti ratios < 39) as a function of Au loading and temperature, we found that as expected, these catalysts exhibited more severe catalyst instability, i.e., increasing the Au loading by a factor of 10 (0.07–0.7 wt%) caused no increase in the PO rate of $17 \pm 2 \times 10^{16}$ molecules/(g s) at 473 K.

Evidence supporting the existence of small Au molecular cluster sites is provided by TEM analysis, where the observable gold particles decorating the TS-1 particles were found to not fully account for the actual gold content of the catalyst, indicating that some of the gold atoms have formed active "invisible" Au–Ti sites. The total number of observable gold atoms per gram of catalyst was estimated by the following procedure. First, we counted the number of gold particles decorating a single TS-1 particle from the TEM micrographs. Assuming hemispherical gold particles, from the number of gold particles per TS-1 particle, one can easily calculate the number of gold atoms per TS-1 particle using the average gold particle diameter; i.e., since the diameter of a gold atom is 2.68×10^{-10} m, approximately 4 atoms can fill the radius of a 2-nm particle, leading to an estimate

of 134 atoms per 2-nm hemispherical gold particle. For a better average, at least 10 TS-1 particles and more than 500 gold particles were analyzed to obtain the number of observable gold atoms per TS-1 particle. The number of observable gold atoms per gram of catalyst was then estimated using the density of TS-1 (~ 1.89 g/cm^3) and the measured effective average TS-1 particle diameter. For this estimation, the TS-1 particles were assumed to be spherical.

A careful analysis for three catalysts with low (~ 0.1 wt%), intermediate (~ 0.5 wt%), and high (~ 0.7 wt%) gold loadings showed that for the low and intermediate loaded catalysts, 88% of gold atoms was not accounted for in the Au particles large enough to be observed using TEM. For the highly loaded gold catalyst, a lower but still sizable percentage of 67% of gold atoms was not accounted for. Interestingly, both the high and the intermediate gold catalysts have very similar unaccounted Au:internal Ti atom ratios of 0.07–0.08 (assuming that for all the gold atoms unaccounted for, one Au atom interacts with one Ti atom), suggesting that the active Au–Ti sites are very limited, and after a gold loading of 0.5 wt%, these sites are effectively saturated. Since the PO rates do not increase proportionally with gold content, it is highly unlikely that the epoxidation occurs at every Au site and/or Au–Ti site. The low gold efficiency is more likely due to a limit in the formation of active Au–Ti sites. As there is an ample number of internal framework Ti sites available (only $\sim 3\%$ of these sites are occupied with 4 Au atoms for a 0.7 wt% gold loaded catalyst), it is unclear what could be limiting the formation of these active sites. Perhaps the active internal Au–Ti site will only preferentially form at Ti sites that are close to a defect as suggested by recent DFT computations [37].

The small (molecular) size of the Au active material suggested by the TEM results is strongly supported by recent DFT calculations showing that a cluster of 3 Au atoms can catalyze a low activation energy pathway for hydrogen peroxide production and that the hydrogen peroxide can, in turn, catalyze PO production at a Ti site in TS-1 [38]. The importance of the hydroperoxy intermediate is further supported by both the experimental observation that supported Au can produce hydrogen peroxide [39] and the direct spectroscopic observation of an OOH intermediate during reaction of H_2 and O_2 on Au/TiO_2 [40]. A question that remains is whether the small Au clusters are on the exterior or interior of the TS-1. Because our gold loadings are so low, there are sufficient exterior Ti sites to accommodate all the gold on the catalysts presented here, and a quantitative assignment of site location is not possible. It seems an unlikely coincidence, however, that the number of external, active Au–Ti sites would be the same when the specific external area, and also the Au surface loading, changes by a factor of 3. Thus, we take the lack of dependence of the TOF on TS-1 particle size as a strong indication of the participation of sites in the interior of the crystallites. Further experiments to address this issue are in progress.

4. Conclusions

1. A study of the effects of DP parameters for Au deposition on TS-1 has shown that DP at pH 9–10 is preferred because this pH allowed for a maximum amount of gold to be deposited, while still maintaining a small average gold particle diameter of 2–5 nm. At this pH, 1–3 wt% of available gold in the solution was consistently deposited onto the conventional TS-1 supports.
2. Depending on the Au loading and extraframework Ti content, our Au/TS-1 catalysts achieved propylene conversions of 2.5–6.5% and PO selectivities of 60–85% at 443 K and a space velocity of 7000 ml g_{cat}^{-1} h^{-1}.
3. Time-dependent kinetic measurements have shown that the stability of the Au/TS-1 catalyst is highly dependent on Au and Ti loading. Dilute Au and Ti systems produce stable and active Au/TS-1 catalysts. For the catalysts that deactivated, an O_2/He treatment at 523 K was unsuccessful in regenerating the catalysts. Since quantitative calculations showed that the carbon that was burned off during the O_2/He treatments was enough to poison the possible Au and Ti sites, it is quite possible that the reaction or the O_2/He treatment conditions caused irreversible rearrangement of the active Au. This rearrangement of the active Au was also evidenced by TEM particle progression experiments where at high Au loading and temperature (473 K), the Au particles grew larger and more Au particles per TS-1 particle were observed. Under these conditions, the PO rates also take a sharp dive, suggesting that the altered state of the Au particles under these conditions corresponds with the instability in reactivity.
4. Similar rates per Au atom for Au on ~ 170 nm TS-1 supports with gold catalysts made from larger particle (519 nm) TS-1 show that the rate does not scale with external surface area and strongly suggest that the active Au–Ti sites are not exclusively the external 2- to 5-nm Au particle/Ti sites suggested in the literature.
5. TEM analysis shows that the observable gold particles decorating the TS-1 particles do not account for the total gold content of the catalyst, indicating that some of the gold atoms have formed “invisible” Au–Ti sites. The ~ 0.7 and ~ 0.5 wt% gold catalysts have very small similar unaccounted Au:internal Ti atom ratios of 0.07–0.08, suggesting that the active Au–Ti sites are very limited in number.

Acknowledgments

The authors thank Jochen Lauterbach, David Wells, Bradley Taylor, and Kendall Thomson for their valuable ideas and discussion, Josh Wilson and Richard Dallinger for the DRUV–vis measurements, and Bradley Taylor for helping to prepare some of the TS-1 supports. We also gratefully acknowledge support for this research by the United

States Department of Energy, Office of Basic Energy Sciences, through Grant DE-FG02-01ER-1510.

References

[1] D.L. Trent, Kirk–Othmer Encyclopedia of Chemical Technology, Wiley, New York, 1996.
[2] K. Weissermel, H.J. Arpe, Industrial Organic Chemistry, VCH, New York, 1993.
[3] Chem. Eng. News 80 (2002) 14.
[4] T. Hayashi, K. Tanaka, M. Haruta, Am. Chem. Soc. Div. Pet. Chem. 41 (1996) 71.
[5] T. Hayashi, K. Tanaka, M. Haruta, J. Catal. 178 (1998) 566.
[6] M. Haruta, B.S. Uphade, S. Tsubota, A. Miyamoto, Res. Chem. Intermed. 24 (1998) 329.
[7] Y.A. Kalvachev, T. Hayashi, S. Tsubota, M. Haruta, Stud. Surf. Sci. Catal. 110 (1997) 965.
[8] Y.A. Kalvachev, T. Hayashi, S. Tsubota, M. Haruta, J. Catal. 186 (1999) 228.
[9] B.S. Uphade, S. Tsubota, T. Hayashi, M. Haruta, Chem. Lett. (1998) 1277.
[10] B.S. Uphade, M. Okumura, S. Tsubota, M. Haruta, Appl. Catal. A 190 (2000) 43.
[11] B.S. Uphade, M. Okumura, N. Yamada, S. Tsubota, M. Haruta, Stud. Surf. Sci. Catal. 130 (2000) 833.
[12] B.S. Uphade, Y. Yamada, T. Akita, T. Nakamura, M. Haruta, Appl. Catal. A 215 (2001) 137.
[13] B.S. Uphade, T. Akita, T. Nakamura, M. Haruta, J. Catal. 209 (2002) 331.
[14] E.E. Stangland, K.B. Stavens, R.P. Andres, W.N. Delgass, J. Catal. 191 (2000) 332.
[15] E.E. Stangland, K.B. Stavens, R.P. Andres, W.N. Delgass, Stud. Surf. Sci. Catal. 130 (2000) 827.
[16] M.G. Clerici, G. Bellussi, U. Romano, J. Catal. 129 (1991) 159.
[17] M.G. Clerici, P. Ingallina, US patent 5221795 (1993).
[18] T.A. Nijhuis, B.J. Huizinga, M. Makkee, J.A. Moulijn, Indust. Eng. Chem. Res. 38 (1999) 884.
[19] A. Kuperman, R. Bowman, H.W. Clark, G.E. Hartwell, B. Schoeman, H.E. Tuinstra, G.R. Meima, International patent WO 00/59632 (2000).
[20] M. Haruta, N. Yamada, T. Kobayashi, S. Ilijima, J. Catal. 115 (1989) 301.
[21] M. Haruta, M. Date, Appl. Catal. A 222 (2001) 427.
[22] M. Haruta, Catal. Today 36 (1997) 153.
[23] M. Haruta, Cattech. 6 (2002) 102.
[24] M.G. Clerici, P. Ingallina, J. Catal. 140 (1993) 71.
[25] S. Tsubota, D.A.H. Cunningham, Y. Bando, M. Haruta, Stud. Surf. Sci. Catal. 91 (1995).
[26] A. Thangaraj, M.J. Aepen, S. Sivasanker, P. Ratnaswami, Zeolites 12 (1992) 943.
[27] A.J.H.P. van der Pol, J.H.C. van der Hooff, Appl. Catal. A 92 (1992) 93.
[28] T. Armaroli, F. Milella, B. Notari, R.J. Willey, G. Busca, Top. Catal. 15 (2001) 63.
[29] E. Duprey, P. Beaunier, M.A. Springuel-Juet, F. Bozon-Verduaz, J. Fraissard, J.M. Manoli, J.M. Breqeault, J. Catal. 165 (1997) 22.
[30] B. Notari, Adv. Catal. 41 (1996) 253.
[31] G. Mul, A. Zwijnenburg, B. van der Linden, M. Makkee, J.A. Moulijn, J. Catal. 201 (2001) 128.
[32] R. Millini, E.P. Massara, G. Perego, G. Bellussi, J. Catal. 137 (1992) 497.
[33] B. Notari, Catal. Today 18 (1993) 163.
[34] M. Taramasso, G. Perego, B. Notari, US patent 4410501 (1983).
[35] M.G. Clerici, U. Romano, US patent 4824976 (1989).
[36] M.G. Clerici, U. Romano, US patent 4937216 (1990).
[37] D.H. Wells, W.N. Delgass, K.T. Thomson, J. Am. Chem. Soc. 126 (2004) 2956.
[38] D.H. Wells, W.N. Delgass, K.T. Thomson, J. Catal. 225 (2004) 69.
[39] P. Landon, P.J. Collier, A.J. Papworth, C.J. Kiely, G.J. Hutchings, Chem. Commun. (2002) 2058.
[40] C. Sivadinarayana, T.V. Choudhary, L.L. Daemen, J. Eckert, D.W. Goodman, J. Am. Chem. Soc. 126 (2004) 38.